Journal of Advanced Research 82 (2026) 1083–1098

Contents lists available at ScienceDirect

Journal of Advanced Research

journal homepage: www.elsevier.com/locate/jare

Original Manuscript

Scutellarein attenuates cancer cachexia-induced muscle atrophy via targeted inhibition of the JAK/STAT pathway

Heeju Ahn [a,1], Heeju Kim [b,1], Yeyoung Yoon [a], Minju Jeong [b], Sieun Lee [c], Peng Chen [d], Keke Wang [e], Sujung Park [a], Jae Hwan Kim [b], Jiyun Ahn [f,g], Qiantao Wang [d], Yoonhee Jin [c], Young Jin Jang [a,*], Sanguine Byun [b,h,**]

[a] Department of Food Science and Technology, Seoul Women's University, Seoul 01797, Republic of Korea
[b] Department of Biotechnology, Yonsei University, Seoul 03722, Republic of Korea
[c] Department of Physiology, Yonsei University College of Medicine, Seoul 03722, Republic of Korea
[d] West China School of Pharmacy, Sichuan University, Chengdu 610041, China
[e] China-US (Henan) Hormel Cancer Institute, Zhengzhou 450003, China
[f] Aging Research Group, Korea Food Research Institute, Wanju-gun 55365, Republic of Korea
[g] Division of Food Biotechnology, University of Science and Technology, Daejeon 34113, Republic of Korea
[h] POSTECH Biotech Center, Pohang University of Science and Technology (POSTECH), Pohang 37673, Republic of Korea

HIGHLIGHTS

- Scutellarein is identified as a potent JAK inhibitor that counteracts cachexia by inhibiting JAK2/STAT3 signaling pathway.
- Scutellarein prevents muscle wasting and enhances mitochondrial function in both cell and animal models.
- Three hydroxyl groups of scutellarein interact with the binding pocket of JAK2, effectively inhibiting its activity.

GRAPHICAL ABSTRACT

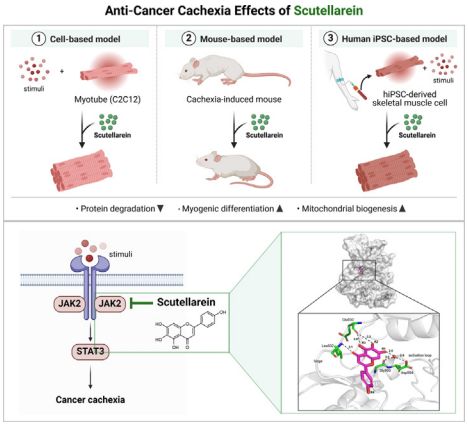

ARTICLE INFO

Article history:
Received 14 April 2025
Revised 9 June 2025
Accepted 2 July 2025
Available online 4 July 2025

Keywords:
Cancer cachexia
Muscle atrophy
Scutellarein

ABSTRACT

Introduction: Cancer cachexia is a multifaceted metabolic syndrome characterized by severe loss of skeletal muscle and adipose tissue, diminishing both quality of life and survival in cancer patients. Despite its prevalence, effective treatments for cancer cachexia remain limited. The JAK/STAT signaling pathway has been identified as a key driver of muscle atrophy in cachexia.
Objectives: This study aimed to investigate the therapeutic potential of scutellarein, a natural compound, as a JAK kinase inhibitor to prevent and mitigate cancer cachexia-induced muscle atrophy.
Methods: *In vitro* experiments were conducted using the mouse myoblast cell line C2C12 and human induced pluripotent stem cell (hiPSC)-derived skeletal muscle cells. Myotube atrophy was induced using IFN-γ/TNF-α and cancer cell-conditioned media. Two independent mouse models of cancer cachexia

* Corresponding author.
** Corresponding author at: Department of Biotechnology, Yonsei University, Seoul 03722, Republic of Korea.
E-mail addresses: jyj@swu.ac.kr (Y.J. Jang), sanguine@yonsei.ac.kr (S. Byun).
[1] These authors made equal contributions to this work.

https://doi.org/10.1016/j.jare.2025.07.001

Janus kinase
Signal transducers and activators of transcription
Skeletal muscle

were utilized for *in vivo* analysis. Muscle tissues were examined through transcriptomic and molecular analyses, including RNA sequencing, PCR, and immunoblotting. Structure-activity relationship studies and molecular docking analyses were performed to investigate the binding interaction of scutellarein with JAK kinases.

Results: Through a chemical library screen, we identified scutellarein as a potent JAK kinase inhibitor. Scutellarein effectively mitigated myotube atrophy by inhibiting protein degradation and promoting protein synthesis in C2C12 and hiPSC-derived muscle cells. In two distinct mouse models of cancer cachexia, scutellarein treatment significantly reduced muscle wasting, improved muscle strength and function, and countered fat depletion. Transcriptomic and molecular analyses of muscle tissues further demonstrated that scutellarein inhibited activation of JAK/STAT pathways and restored suppression of myogenesis and mitochondrial biogenesis. Structure-activity relationship analyses further revealed critical hydroxyl group positions essential for JAK binding.

Conclusion: Collectively, our findings suggest scutellarein as a promising candidate for the prevention and treatment of cancer cachexia, providing a novel therapeutic approach to address this critical unmet need in cancer care.

Introduction

Cancer cachexia is a multifaceted metabolic syndrome characterized by significant weight loss in both skeletal muscle and adipose tissue [1,2]. Recently, muscle mass depletion has become recognized as the primary characteristic of the condition [3]. This condition is distinct from other forms of muscle loss, such as those caused by starvation, aging, depression, or malabsorption. About 50% of cancer patients suffer from cachexia, leading to diminished quality of life and shortened survival times [4]. Notably, even a weight loss of 2% has been associated with marked decrease in quality of life [5]. Therefore, understanding and effectively managing cachexia is crucial for improving outcomes and extending survival of patients [4]. Despite its widespread impact, there is currently no standardized treatment available to prevent or treat cachexia. This underscores the need to discover new therapeutics to address this fatal syndrome.

To combat muscle atrophy in cancer cachexia, it is imperative to target the key signaling pathways that drive its pathogenesis. Unlike muscle atrophy caused by starvation or physical inactivity, muscle wasting seen in cachectic patients cannot be reversed through nutritional supplementation [6]. The primary molecular mechanisms underlying cachexia involve decreased protein synthesis and increased protein degradation, where signaling pathways activated by pro-inflammatory cytokines such as TNF-α, IFN-γ, and IL-6 play a key role in driving this condition [7–9]. These cytokines increase in serum of patients suffering from cachexia as well as cachectic mouse models [10,11]. Among several downstream signaling pathways triggered by them, activation of JAK/STAT3 in skeletal muscle was identified to play a significant role in cancer-induced muscle atrophy through systemic inflammatory response [9,12]. Several studies identified that inhibition of JAK/STAT3 pathway attenuates cachexia-associated muscle and adipose wasting [13,14]. Therefore, therapeutic targeting of JAK presents a potential strategy for modulating cancer cachexia.

Natural compounds have long been a significant source of bioactive leads in drug discovery [15]. Given their importance, we sought to identify a natural compound capable of inhibiting JAK for potential application in the treatment of cachexia. In this study, we screened 684 natural compounds for their inhibitory effects on JAK activity and identified scutellarein as a top candidate. Scutellarein, a flavonoid monomer found in herbs like *Scutellaria baicalensis* and *Erigeron breviscapus*, has been reported for its anti-inflammatory, antioxidant, and anti-diabetic properties [16–18]. Despite its therapeutic potential, scutellarein's effects on cancer cachexia and muscle atrophy have not been previously studied and remain unexplored. Therefore, we demonstrated potent inhibitory effects of scutellarein across all JAK kinases (JAK1, JAK2, JAK3, and TYK2), with further analysis revealing direct molecular inhibition against JAK2. By targeting JAK2, scutellarein effectively attenuated and prevented cancer cachexia in both cellular and animal models.

Materials and methods

Reagents

Scutellarein was obtained from Selleck Chemicals LLC (Houston, TX, USA) and ChemFaces Biochemical Co., Ltd. (Wuhan, China), and dimethyl sulfoxide (DMSO) was purchased from TCI Chemicals (Tokyo, Japan). Recombinant murine IFN-γ and TNF-α were purchased from PeproTech (Cranbury, NJ, USA). Baicalein and apigenin were acquired from Cayman Chemical (Ann Arbor, MI, USA), while chrysin and 4′,6-dihydroxyflavone were sourced from Sigma-Aldrich (St. Louis, MO, USA). 4′,7-dihydroxyflavone and 4′,5-dihydroxyflavone were obtained from MedChemExpress (MCE) (Monmouth Junction, NJ, USA). Additionally, 5,6-dihydroxyflavone was supplied by Alfa Aesar (Ward Hill, MA, USA), and 6,7-dihydroxyflavone was acquired from Biosynth (Staad, Switzerland).

Details regarding antibodies used are given in the Supplemental Materials and Methods.

Kinase and binding assays

Multiple kinase assays were performed to evaluate the kinase activity of JAK kinases and assess the binding affinity between scutellarein and JAK kinases. Details regarding kinase and binding assays are given in the Supplemental Materials and Methods.

Molecular docking

Molecular docking was conducted using AutoDock Vina to predict the binding pose of scutellarein with JAK2 protein [19]. Details regarding molecular docking are given in the Supplemental Materials and Methods.

Cell culture

Details regarding cell culture are given in the Supplemental Materials and Methods.

CT26 conditioned medium (CCM) preparation

The CT26 cell line, a murine colon carcinoma derived from BALB/c mice, was utilized to model the progression of colorectal

cancer. These cells were obtained from the Korean Cell Line Bank (Seoul, Republic of Korea) and cultured to simulate cachexia observed in cancer. For the preparation of conditioned medium, CT26 cells were grown in standard growth medium until they reached approximately 80% confluence. Subsequently, the medium was switched to serum-free DMEM to initiate the conditioning phase. After 48 hours, the medium was harvested and centrifuged to eliminate any cellular debris, followed by sterile filtration using a 0.2 μm syringe filter to ensure the removal of all particulate matter.

Cell viability assays

Details regarding cell viability assays are given in the Supplemental Materials and Methods.

Immunoblotting

Details regarding immunoblotting are given in the Supplemental Materials and Methods.

Immunofluorescence

Details regarding immunofluorescence are given in the Supplemental Materials and Methods.

Quantitative real-time polymerase chain reaction

Details regarding quantitative real-time polymerase chain reaction (qRT-PCR) are given in the Supplemental Materials and Methods.

Surface sensing of translation (SUnSET) assay

The SUnSET assay, a nonradioactive technique, was employed to monitor changes in protein synthesis by tracking the incorporation of puromycin into nascent peptide chains in mammalian cells [20]. In this protocol, C2C12 murine myoblasts were treated with varying concentrations of scutellarein. During the final hour of treatment, puromycin was added at a concentration of 1 μM to facilitate its incorporation into newly synthesized proteins. The extent of puromycin incorporation was then analyzed via western blotting to quantify the rate of protein synthesis.

Immunocytochemical staining

Details regarding immunocytochemical staining are given in the Supplemental Materials and Methods.

Measurement of mitochondrial oxygen consumption rate (OCR)

Mitochondrial respiration was assessed by measuring the OCR using the XF96 Extracellular Flux Analyzer (Seahorse Bioscience, MA, USA). Details regarding its measurement are given in the Supplemental Materials and Methods.

Mouse studies and behavioral tests

Details regarding mouse studies and behavioral are given in the Supplemental Materials and Methods.

Histopathological analysis

To evaluate the histological features of the mouse gastrocnemius muscle, Hematoxylin and Eosin (H&E) staining was performed, following methods adapted from previous [21]. The muscle tissue was preserved in 4% paraformaldehyde, then sectioned at a thickness of 7 μm. Each section was stained using commercially available Harris Hematoxylin and Eosin solutions. Following staining, the tissue sections were examined under an Olympus CKX53 microscope to ensure quality and consistency. The cross-sectional area (CSA) of the muscle fibers was precisely quantified using ImageJ software.

RNA sequencing (RNA-seq) and analysis

Details regarding RNA sequencing (RNA-seq) and analysis are given in the Supplemental Materials and Methods.

Statistical analysis

Experimental data are presented as mean ± standard deviation (SD) for *in vitro* studies and as mean ± standard error of the mean (SEM) for *in vivo* studies. Details regarding statistical tests used for datasets are given in Supplemental Material and Methods. All statistical analyses were conducted using GraphPad Prism software, version 8.0.1 (GraphPad Software, La Jolla, CA, USA). Values of $p < 0.05$ were considered statistically significant.

Results

Identification of scutellarein as an inhibitor against JAK kinases

To identify compounds with inhibitory activity against JAK1, we performed a library screening of 684 natural compounds (Fig. 1A). The top 1% of compounds showing the highest inhibitory activity in the kinase assay were selected as hits. The hit compounds were subsequently screened against JAK1, JAK2, JAK3, and TYK2 activity, and cytotoxicity assays were conducted. Compounds lacking therapeutic applicability or novelty were excluded and scutellarein was chosen for further investigation (Fig. 1B, C). To examine the detailed relationship between scutellarein and JAK kinases, IC_{50} values were determined. Scutellarein effectively reduced the activity of JAK2, JAK3, and TYK2 *in vitro*, without exerting any cytotoxic effects (Fig. 1D, Supplementary Fig. 1). The JH1 domain is the kinase domain, responsible for phosphorylating downstream substrates such as STAT3 [22]. To further explore the interaction of scutellarein with JAK kinases, a binding assay was used to assess scutellarein's binding affinity to the JH1 domain of various JAK proteins. The results show potent binding affinity to JAK kinases as indicated by the Kd values (Fig. 1E). Furthermore, to validate its specificity, the effects of scutellarein on four additional kinases – EGFR, IGF1R, p38α, and ERK1 – were evaluated (Fig. 1F). The first two are receptor tyrosine kinases (RTKs), while p38α and ERK1 are part of the mitogen-activated protein kinase (MAPK) family. In comparison to JAK2, scutellarein exhibited minimal inhibitory activity against these kinases, further confirming its specificity for JAK kinases. These findings collectively suggest that scutellarein is a potent inhibitor of JAK kinases.

Scutellarein protects against IFN-γ/TNF-α-induced myotube atrophy in C2C12 cells

In cancer cachexia, tumor-secreted pro-inflammatory cytokines, such as IFN-γ and TNF-α, induce muscle wasting [23]. These cytokines synergistically induce myotube atrophy by activating the JAK2/STAT3 pathway, which enhances protein degradation and suppresses muscle differentiation factors [8,9,24,25]. First, we examined whether scutellarein could attenuate the IFN-γ/TNF-α-induced JAK2/STAT3 pathway in cells. We observed significant activation of the pathway in response to IFN-γ/TNF-α. Nota-

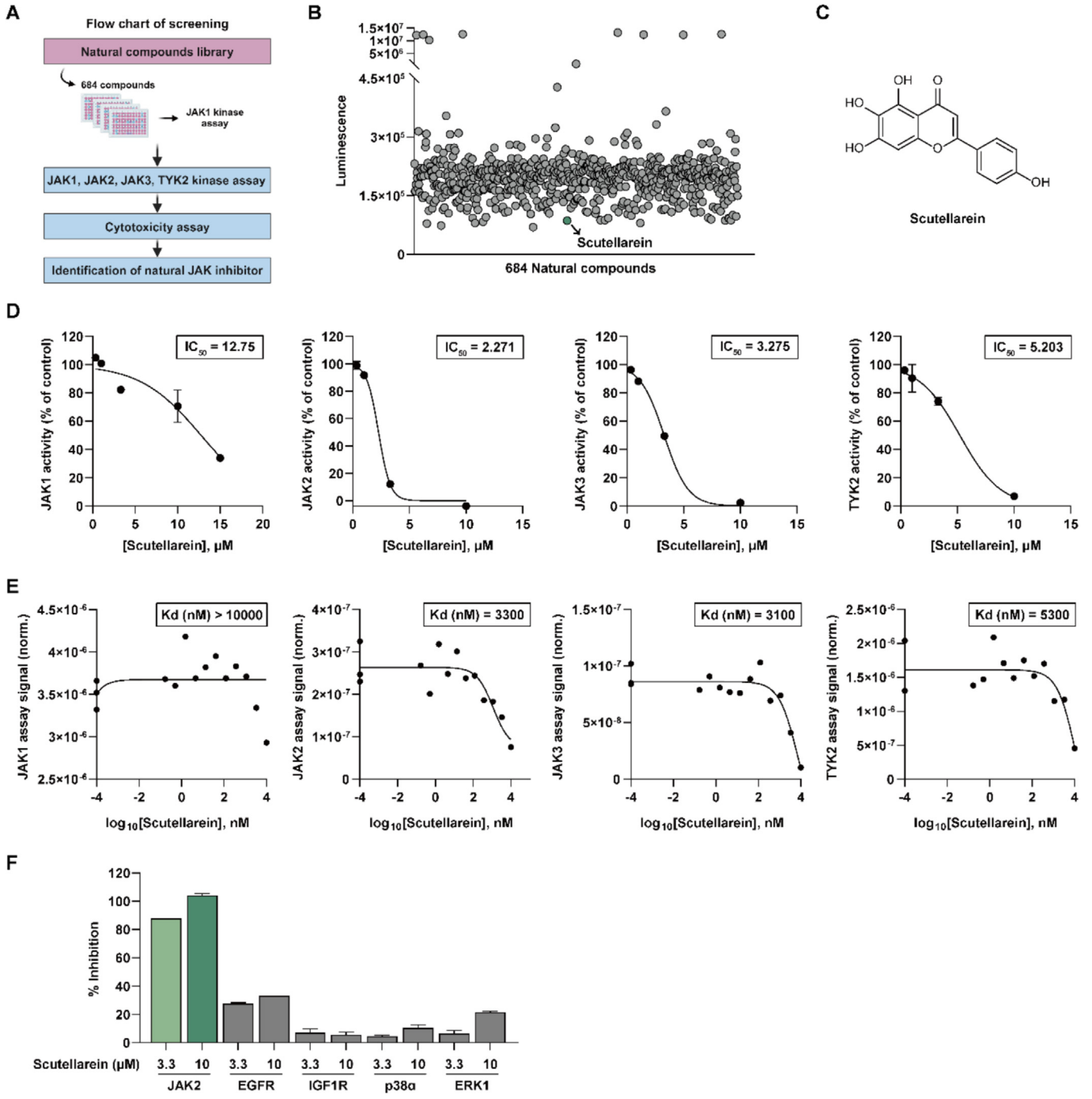

Fig. 1. Identification of scutellarein as a JAK kinase inhibitor and *in vitro* validation. (A) Schematic representation of the screening process. A library of 684 natural compounds was screened for inhibitory activity against JAK kinases. Hits were validated and further confirmed through *in vitro* assays. (B) Inhibitory activity of 684 natural compounds against JAK1 was measured using the ADP-Glo™ kinase assay. (C) Chemical structure of scutellarein. (D) Dose-response curves for scutellarein's inhibition of all four JAK kinases (JAK1, JAK2, JAK3, and TYK2) are presented, as measured by kinase assays. IC_{50} values were calculated using GraphPad Prism software, version 8.0.1. (E) Eurofins binding assay results showing the binding affinity (Kd values) of scutellarein for the JH1 domain of the JAK kinases. (F) Inhibitory effects of scutellarein on EGFR, IGF1R, p38α, and ERK1 assessed using kinase assays. Scutellarein was tested at concentrations of 3.3 μM and 10 μM.

bly, scutellarein effectively inhibited the activation of both JAK2 and STAT3 (Fig. 2A and B). This suppression of the JAK2/STAT3 pathway suggests that scutellarein can directly target this signaling pathway in cells. Since scutellarein inhibits JAK kinases, we further examined its impact on other downstream factors of JAK signaling. Specifically, we analyzed STAT5, a known downstream target of JAK2 [26]. Treatment with pro-inflammatory cytokines resulted in STAT5 phosphorylation; however, the addition of scutellarein effectively inhibited this phosphorylation, confirming that scutellarein suppresses JAK activity and, consequently, its downstream signaling (Fig. 2B). To assess the specificity of this inhibition, we examined other signaling pathways, including JNK, p38, NF-κB and TAK. Their phosphorylated forms increased due to treatment of IFN-γ/TNF-α, but remain unchanged after treatment with scutellarein, suggesting that scutellarein selectively targets the JAK2/STAT axis (Fig. 2C, Supplementary Fig. 2A). Next, to

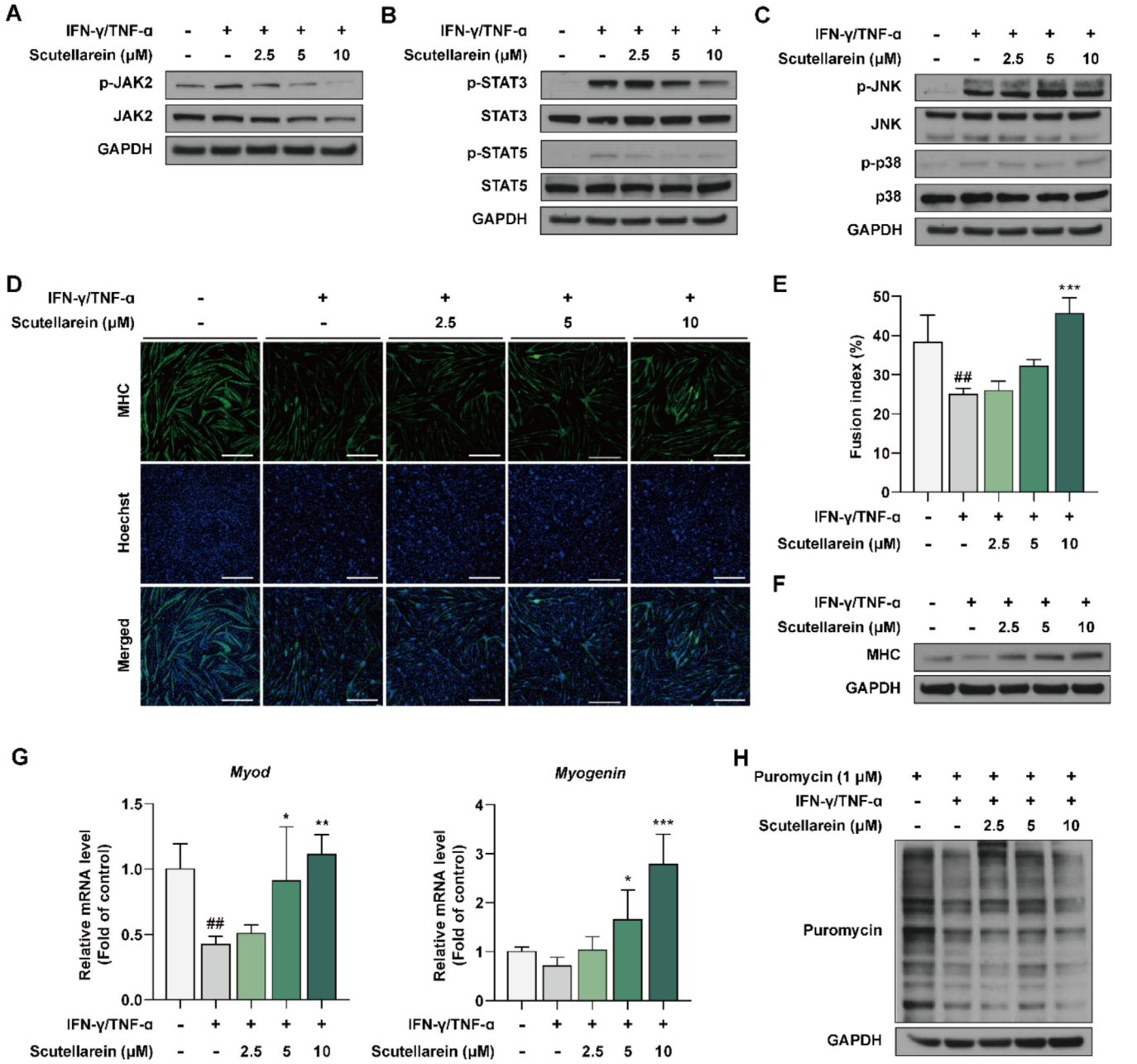

Fig. 2. Scutellarein protects against IFN-γ/TNF-α-induced myotube atrophy in C2C12 cells. Myotubes were treated with indicated concentrations of scutellarein and inflammatory cytokines, IFN-γ (20 ng/mL) and TNF-α (20 ng/mL). (A-C) Expression levels of phosphorylated and total JAK2 (A), STAT3, STAT5 (B), JNK, and p38 (C) were analyzed by immunoblotting. (D) Representative immunofluorescence images of MHC (green), Hoechst (blue), and merged images are shown, and (E) fusion index was quantified using ImageJ software. Scale bar: 200 μm. (F) Protein expression levels of MHC analyzed by immunoblotting. (G) mRNA expression of MyoD and myogenin was evaluated by qRT-PCR. (H) Protein synthesis following 24-hour treatment of scutellarein and IFN-γ/TNF-α was assessed using the SUnSET assay, with puromycin incorporation visualized by immunoblotting. GAPDH was used as a loading control. The data are presented as mean ± SD (n = 4–5). Statistical significance was determined by one-way ANOVA followed by Dunnett's multiple comparisons test. ## $p < 0.01$ vs. control group; * $p < 0.05$, ** $p < 0.01$, and *** $p < 0.001$ vs. IFN-γ/TNF-α group. (For interpretation of the references to colour in this figure legend, the reader is referred to the web version of this article.)

investigate the protective effects of scutellarein against muscle atrophy associated with cachexia, we performed a series of experiments using C2C12 myotubes treated with IFN-γ and TNF-α. C2C12 myoblasts were fully differentiated into myotubes prior to treatment with scutellarein. To model cachexia-induced muscle atrophy, cells were exposed to cytokines, and the impact of scutellarein on IFN-γ/TNF-α-induced myotube atrophy was subsequently assessed. The morphological changes associated with myosin heavy chain (MHC) expression were assessed through immunofluorescence microscopy. Myotubes exhibited significant shrinkage upon cytokine treatment, whereas co-treatment with scutellarein effectively prevented this atrophy, demonstrating its effect in muscle preservation (Fig. 2D). We evaluated the fusion index, a widely used metric in muscle cell culture assays to estimate myocyte fusion [27]. Results demonstrate that treatment with scutellarein effectively prevented the IFN-γ/TNF-α-mediated repression of myocyte fusion in a dose-dependent manner and increased MHC protein expression (Fig. 2E and F). In addition, the mRNA expression levels of MyoD and myogenin, two critical regulators of myoblast differentiation, were examined [28,29]. IFN-γ/

TNF-α-induced suppression of MyoD and myogenin was restored by scutellarein treatment (Fig. 2G). This restoration of differentiation markers suggests that scutellarein preserves muscle structure and myogenic potential. Consistently, treatment with JAK family inhibitors, ruxolitinib and tofacitinib, also upregulated the expression of MyoD, myogenin, and MHC (Supplementary Fig. 2B, C). To further elucidate the effects of scutellarein on protein synthesis, the SUnSET assay was conducted. Scutellarein attenuated the suppression of protein synthesis mediated by IFN-γ/TNF-α treatment (Fig. 2H), indicating its role in maintaining protein synthesis in muscle cells under inflammatory stress. Collectively, these findings indicate that scutellarein not only preserves myocyte fusion and differentiation but also protects against protein synthesis suppression and myotube atrophy by inhibiting the JAK2/STAT3 signaling pathway.

Scutellarein prevents cancer cell-conditioned medium-induced myotube atrophy in C2C12 cells

Following our investigation of myotube atrophy induced by IFN-γ and TNF-α, we next examined the effects of scutellarein on myotube atrophy induced by conditioned medium from cancer cells. C2C12 myoblast cells were exposed to CT26 colon carcinoma cell-conditioned medium (CT26-CM) to mimic the cancer cachexia microenvironment, and the impact of scutellarein on CT26-CM-induced myotube atrophy was assessed. Scutellarein significantly ameliorated CT26-CM-induced myotube atrophy, as evidenced by an increased fusion index and higher protein expression levels of MHC (Fig. 3A–C). These findings suggest that scutellarein exerts a protective effect on muscle structure in the cancer cachexia model, promoting muscle cell differentiation and fiber integrity. Additionally, scutellarein reduced the expression of the muscle-specific ubiquitin ligases MAFbx and MuRF1, which were markedly upregulated in response to CT26-CM treatment (Fig. 3D). These ligases are key regulators of protein degradation in muscle cells [30]. Indeed, scutellarein prevented CT-26-CM-mediated suppression of protein synthesis (Fig. 3E). Furthermore, it suppressed the elevated phosphorylation levels of JAK2 and STAT3, demonstrating its ability to inhibit the JAK2/STAT3 signaling pathway in the CT26-CM environment (Fig. 3F). Previous research has demonstrated that inhibition of the JAK/STAT3 signaling pathway suppresses the expression of MAFbx and MuRF1, while elevating MHC content in denervated tibialis anterior muscles [31]. In line with this, our data suggest that scutellarein exerts a protective effect against CT26-CM-mediated myotube atrophy in C2C12 myoblast cells by modulating the JAK2/STAT3 pathway.

Scutellarein prevents cancer cachexia in a CT26 tumor model

Following our cellular experiments, we evaluated the effects of scutellarein on cancer cachexia in a CT26-induced cachexia model using BALB/c mice. The mice were given *ad libitum* access to either a standard diet or a standard diet supplemented with scutellarein (24 mg/kg) for 10 weeks. To induce cancer cachexia, CT26 colon carcinoma cells were subcutaneously injected into the right flank during the last two weeks of treatment. Mice were euthanized at the end of the study for analysis (Fig. 4A). Behavioral experiments demonstrated reduced muscle strength and exercise performance in cancer cachexia-induced mice. However, the scutellarein-treated group exhibited significantly greater running distance and time (Fig. 4B). The decline in Kondziela test hanging time and grip strength was also effectively prevented by scutellarein treatment, suggesting recovery of muscle function (Fig. 4C and D). Muscle mass significantly decreased in cancer cachexia-induced mice, while scutellarein-treated mice maintained muscle weight comparable to that of tumor-free controls, as examined in triceps, quadriceps, tibialis anterior (TA), extensor digitorum longus (EDL), gastrocnemius, and soleus muscles (Fig. 4E–K). However, tumor mass between the two tumor-bearing groups showed no significant difference, indicating that scutellarein's effects were specific to muscle preservation (Fig. 4L). Furthermore, the mass of inguinal white adipose tissue (iWAT) was also restored in scutellarein-treated mice (Fig. 4M). Therefore, tumor-free body weight increased compared to cancer cachexia-induced mice, and scutellarein did not significantly affect the weights of the liver and heart. (Supplementary Fig. 3A–C). Hematoxylin and eosin (H&E) staining of the gastrocnemius muscles revealed a reduction in muscle fiber cross-sectional area (CSA) and an increased frequency of smaller fibers in response to cachexia development (Fig. 4N–P). Notably, scutellarein prevented these atrophic changes in muscle fibers.

Protein expression analysis of quadricep muscles revealed increased phosphorylation of STAT3, whereas scutellarein consumption led to a reduction in STAT3 phosphorylation levels (Fig. 4Q, Supplementary Fig. 3D). In quadricep muscles, elevated levels of muscle atrophy markers MAFbx and MuRF1 were observed, along with decreased MHC expression from CT26-injected mice. These detrimental effects were significantly mitigated by scutellarein treatment (Fig. 4R, Supplementary Fig. 3E). We also examined the downstream regulators of the mTORC1 signaling pathway, which plays a crucial role in muscle protein synthesis and cell growth [32,33]. Phosphorylation levels of downstream effector molecules of mTORC1, p70S6K and 4E-BP1, were suppressed in cancer cachectic muscles but were restored following scutellarein treatment, indicating a recovery of the protein synthesis signaling pathway (Fig. 4S and Supplementary Fig. 3F). Similarly, markers of mitochondrial biogenesis, such as AMPK, Sirt1, PGC1α, and PPARδ were elevated in scutellarein-treated mice, suggesting improved mitochondrial function (Fig. 4T and Supplementary Fig. 3G) [34,35]. Additionally, the expression of four ubiquitin ligase genes, including *Mafbx*, *Trim63*, *Musa1*, *Fbxo31*, was upregulated in cachectic muscles and significantly reduced by scutellarein (Fig. 4U) [36,37]. To further confirm the effect of scutellarein on mitochondrial biogenesis, we conducted additional experiments using C2C12 myoblasts. Scutellarein treatment reversed the IFN-γ/TNF-α-mediated downregulation of key mitochondrial regulators, including PGC-1α, Sirt1, Opa1, Mfn2, ATP5a1, and UQCRC1 (Supplementary Fig. 4A). Additionally, Mito-Tracker staining revealed that conditioned medium from CT26 cells (CT26-CM) markedly reduced mitochondrial content in C2C12 myotubes, which was substantially rescued by scutellarein treatment (Supplementary Fig. 4B). Seahorse XF analysis showed that IFN-γ/TNF-α treatment significantly reduced the oxygen consumption rate (OCR) in C2C12 myotubes, indicating a marked suppression of basal and maximal respiration. However, co-treatment with scutellarein (2.5, 5, and 10 μM) dose-dependently restored OCR values toward control levels, effectively rescuing the mitochondrial dysfunction induced by the cytokines (Supplementary Fig. 4C and D). In cancer cachexia, lipolysis is also significantly upregulated by the JAK/STAT3 pathway, leading to rapid adipose tissue depletion [38]. This continuous fat breakdown severely impacts patient health. Previous research demonstrates that JAK inhibitors can effectively suppress cachexia-associated adipose wasting [14]. In our findings, STAT3 was activated in the iWAT of cachectic mice, and treatment with scutellarein significantly reduced STAT3 phosphorylation (Fig. 4V and Supplementary Fig. 3H). UCP1, a key protein involved in mitochondrial heat production and fatty acid oxidation, was also upregulated by cachexia and restored by scutellarein (Fig. 4V and Supplementary Fig. 3H) [39]. These results suggest that scutellarein counteracts adipose wasting in cancer cachexia by inhibiting the JAK2/STAT3 pathway. Overall, scutellarein helps prevent cancer cachexia by preserving

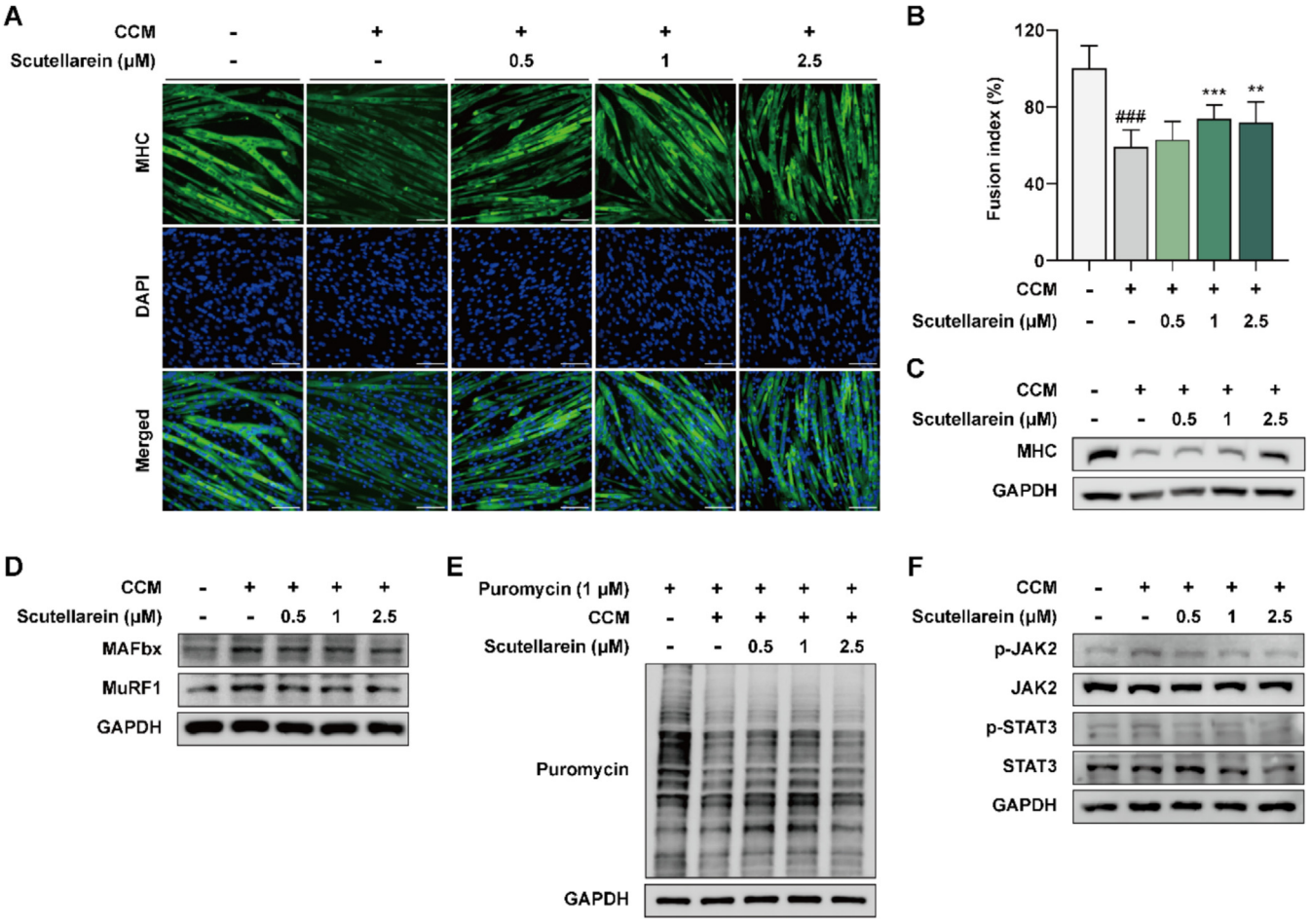

Fig. 3. Scutellarein attenuates CT26-CM-induced myotube atrophy in C2C12 cells. Myotubes were treated with indicated concentrations of scutellarein and CT26-CM. (A) Representative immunofluorescence images of MHC (green), DAPI (blue), and merged images are shown, and (B) fusion index was quantified using ImageJ software. Scale bar: 50 μm. Protein expression levels of (C) MHC, (D) MAFbx and MuRF1, (E) puromycin, and (F) phosphorylated and total JAK2 and STAT3 were analyzed by immunoblotting. GAPDH was used as a loading control. The data are presented as mean ± SD (n = 4–5). Statistical significance was determined by one-way ANOVA followed by Dunnett's multiple comparisons test. ### $p < 0.001$ vs. control group; ** $p < 0.01$, and *** $p < 0.001$ vs. CCM group. (For interpretation of the references to colour in this figure legend, the reader is referred to the web version of this article.)

muscle and adipose tissue, improving muscle strength and performance, and enhancing both protein synthesis and mitochondrial biogenesis.

Scutellarein attenuates cancer cachexia in a Lewis lung carcinoma model

To further investigate the effects of scutellarein on established cancer cachexia, we employed a second animal model with Lewis lung carcinoma (LLC)-induced cachexia in C57BL/6 mice. LLC cells were subcutaneously injected into the right flank, and scutellarein was orally administered three times a week (24 mg/kg), beginning four days after tumor implantation, when visible tumors had formed. The experiment continued for a total of 18 days, with endpoint analyses performed at the conclusion of this period (Fig. 5A). Consistent with the CT26-induced model, LLC-induced cachexia led to reductions in physical strength, muscle mass, and regulatory protein expressions. Behavioral tests, including treadmill performance, hanging time, and grip strength, were diminished but significantly improved following scutellarein treatment (Fig. 5B–D). This demonstrates that scutellarein administration restores muscle strength and function even when introduced after tumor development. Upon sacrifice, triceps, quadriceps, TA, EDL, gastrocnemius, soleus muscles and white adipose tissue weights were significantly higher in scutellarein-treated mice compared to the cachexia group, while tumor mass remained unaffected (Fig. 5E–M). Excluding the tumor, body weight was significantly increased in the scutellarein-treated group compared to the cachexia group (Supplementary Fig. 5Supplementary Fig. 5A). Additionally, scutellarein treatment did not affect the weights of the liver and heart (Supplementary Fig. 5B and C). Improvements in muscle mass and function were further confirmed through histological analysis. H&E staining revealed an increase in muscle fiber cross-sectional area (CSA) in scutellarein-treated mice compared to their cachectic mice counterpart (Fig. 5N). Quantitative analysis showed a higher frequency of large CSA fibers and an increase in average CSA in response to scutellarein treatment (Fig. 5O and P). Protein expression analysis of quadricep muscles showed elevated STAT3 phosphorylation in LLC-injected mice, which was reduced by scutellarein (Fig. 5Q and Supplementary Fig. 5D). Additionally, the expression of ubiquitin ligases MAFbx and MuRF1 increased, while MHC expression decreased in LLC-injected mice. These effects were mitigated by scutellarein (Fig. 5R and Supplementary Fig. 5E). The expression of ubiquitin ligases, which was elevated in cachexia, was also suppressed by scutellarein (Fig. 5S). In iWAT, STAT3 phosphorylation was markedly reduced by scutellarein treatment (Fig. 5T and Supplementary Fig. 5F). In conclusion, our findings suggest that scutellarein has the capacity to both prevent

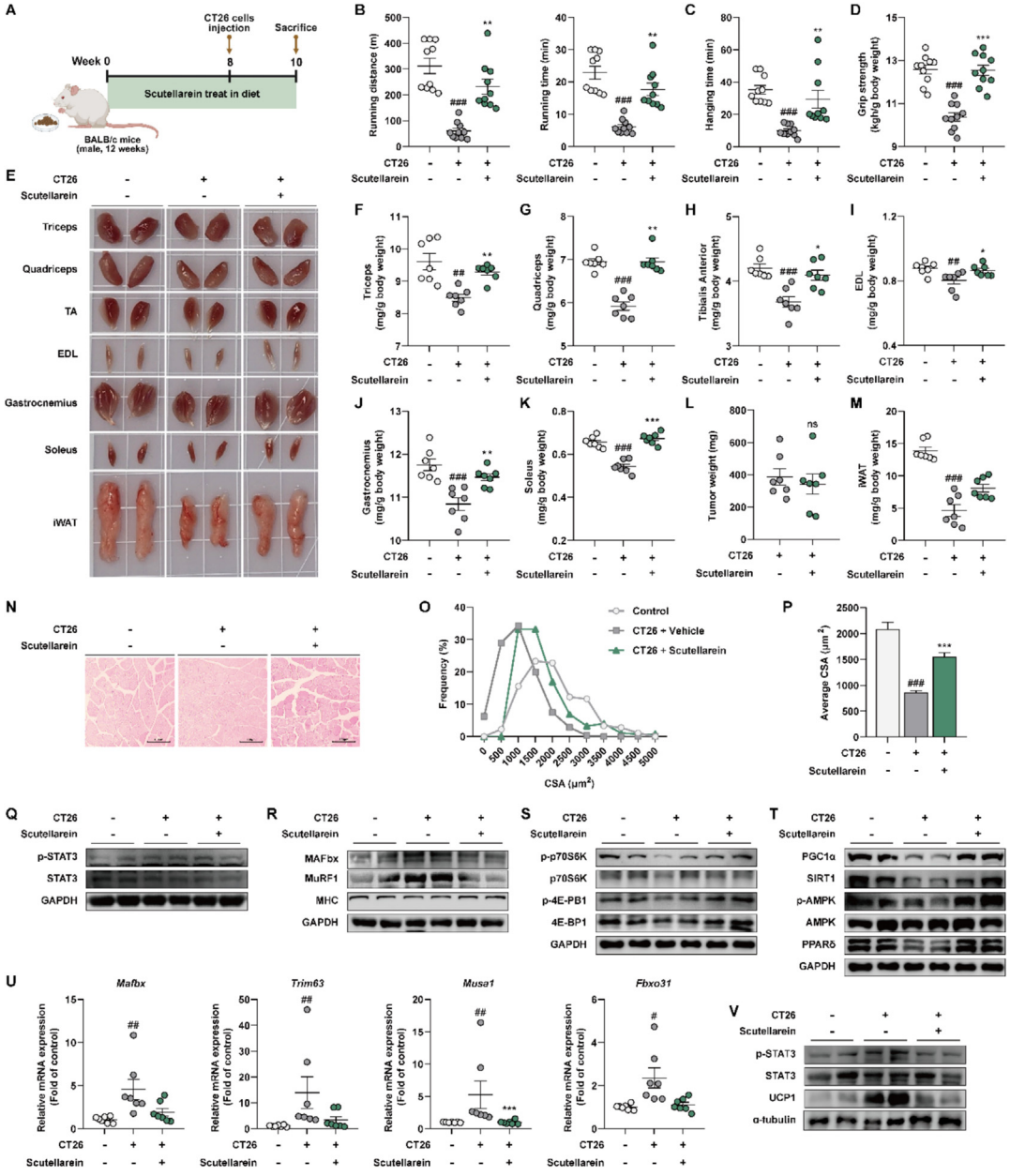

Fig. 4. Scutellarein prevents CT26-induced cancer cachexia in BALB/c mice. (A) Experimental schematic of the CT26-induced cancer cachexia model. BALB/c mice were supplemented with the AIN-93G diet containing scutellarein (24 mg/kg) for 10 weeks. In the final 2 weeks, CT26 colon carcinoma cells (1×10^6) were subcutaneously injected to induce cancer. Mice were euthanized at the end of the 10-week period for analysis. (B-D) Behavioral test results: (B) Treadmill test showing running distance and time, (C) hanging time in Kondziela's inverted screen test, and (D) weekly grip strength measurements. (E) Representative images of skeletal muscles and adipose tissues. (F-M) Quantification of tissue weights: (F) triceps, (G) quadriceps, (H) tibialis anterior (TA), (I) extensor digitorum longus (EDL), (J) gastrocnemius, (K) soleus muscles, (L) tumor and (M) inguinal white adipose tissue (iWAT). (N) Representative H&E staining images of muscle cross-sectional area (CSA). Scale bar: 100 μm. (O) Frequency distribution of muscle fiber CSA. (P) Average muscle fiber CSA (μm^2). (Q-T) Immunoblot analysis of protein expressions in quadriceps muscles: (Q) p-STAT3/STAT3, (R) MHC, MAFbx, MuRF1, (S) p-p70S6K/p70S6K, p-4E-BP1/4E-BP1, and (T) PGC1α, SIRT1, p-AMPK/AMPK, PPARδ. GAPDH was used as a loading control. (U) mRNA expression levels of *Mafbx*, *Trim63*, *Musa1*, and *Fbxo31* in quadriceps muscles analyzed by qRT-PCR. (V) Immunoblot analysis of p-STAT3/STAT3 and UCP1 in iWAT. α-tubulin was used as a loading control. Data are presented as mean ± SEM ($n \geq 7$). Statistical significance was determined by original one-way ANOVA or Kruskal-Wallis test followed by Dunnett's multiple comparisons test. ns, not significant; # $p < 0.05$, ## $p < 0.01$, and ### $p < 0.001$ vs. control group; * $p < 0.05$, ** $p < 0.01$, and *** $p < 0.001$ vs. CT26 group.

and treat cancer cachexia. In the CT26 model, scutellarein functioned as a preventive agent, maintaining muscle mass and function before cachexia fully developed. In contrast, in the LLC model, scutellarein exhibited therapeutic effects, ameliorating established cachexia by restoring muscle strength, mass, and function. This dual action highlights the potential of scutellarein as a versatile therapeutic strategy for addressing cancer cachexia both prophylactically and after onset.

Transcriptomic analysis reveals JAK/STAT pathway inhibition in cachectic muscle by scutellarein

Using the LLC-induced cancer cachexia mouse model, we performed transcriptome profiling in quadricep muscles using RNA sequencing to investigate the transcriptional effects of scutellarein. Principal Component Analysis (PCA) and heatmap clustering revealed distinct segregation of gene expression profiles, with

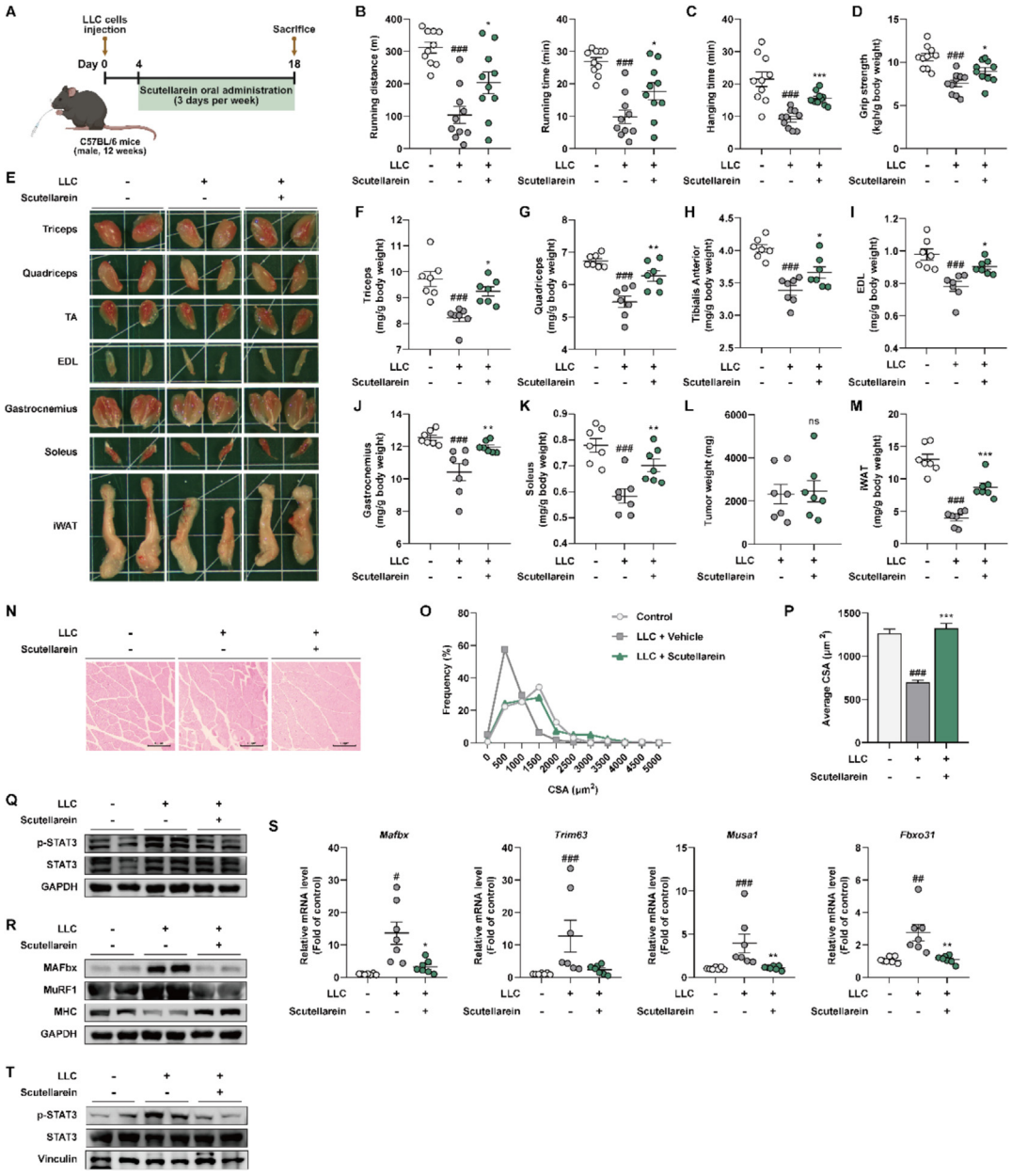

Fig. 5. Scutellarein ameliorates LLC-induced cancer cachexia in C57BL/6 mice. (A) Experimental schematic for the LLC-induced cancer cachexia model. C57BL/6 mice were inoculated with 1×10^6 LLC lung carcinoma cells, which were subcutaneously injected into the right flank. Scutellarein was orally administered three times per week, starting four days after inoculation, when visible tumors appeared. (B-D) Behavioral test results: (B) Treadmill test showing running distance and time, (C) hanging time in Kondziela's inverted screen test, and (D) weekly grip strength measurements. (E) Representative images of skeletal muscles and adipose tissues. (F-M) Quantification of tissue weights: (F) triceps, (G) quadriceps, (H) tibialis anterior (TA), (I) extensor digitorum longus (EDL), (J) gastrocnemius, (K) soleus muscles, (L) tumor and (M) inguinal white adipose tissue (iWAT). (N) Representative H&E staining images of muscle cross-sectional area (CSA). Scale bar: 100 μm. (O) Frequency distribution of muscle fiber CSA. (P) Average muscle fiber CSA (μm^2). (Q-R) Immunoblot analysis of protein expression in quadriceps muscles: (Q) p-STAT3/STAT3 and (R) MHC, MAFbx, and MuRF1. GAPDH was used as a loading control. (S) mRNA expression levels of *Mafbx*, *Trim63*, *Musa1*, and *Fbxo31* in quadriceps muscles analyzed by qRT-PCR. (V) Immunoblot analysis of p-STAT3/STAT3 in iWAT. Vinculin was used as a loading control. Data are presented as mean ± SEM ($n \geq 7$). Statistical significance was determined by original one-way ANOVA, Brown-Forsythe and Welch ANOVA, or Kruskal-Wallis test followed by Dunnett's multiple comparisons test. ns, not significant; # $p < 0.05$, ## $p < 0.01$, and ### $p < 0.001$ vs. control group; * $p < 0.05$, ** $p < 0.01$, and *** $p < 0.001$ vs. LLC group.

cachectic group clustering separately from the control group, indicating significant transcriptomic alterations (Fig. 6A and B). Importantly, scutellarein treatment reversed the overall gene expression patterns in the muscle, resulting in a profile similar to the control group (Fig. 6A and B). To identify significantly enriched signaling and hallmark pathways affected by cachexia and scutellarein treatment, Gene Set Enrichment Analysis (GSEA) was conducted (Fig. 6C). Consistent with previous studies, a marked enrichment in pathways associated muscle atrophy were observed in cachectic muscles, including apoptosis, hypoxia, and proteasome activation [7,40]. Additionally, cancer-induced inflammatory pathways that cause muscle atrophy were significantly activated in cachectic muscle but suppressed by scutellarein treatment. Conversely, genes upregulated by scutellarein were predominantly associated with myogenesis, suggesting a potential protective or regenerative role. Among inflammatory pathways, the JAK/STAT3 pathway was significantly enriched in cachectic muscles. Specifically, the LLC group exhibited a significant upregulation of this pathway compared to the control group, as indicated by the positive running enrichment score (NES > 1.5, P < 0.01) (Fig. 6D). In contrast, the scutellarein-

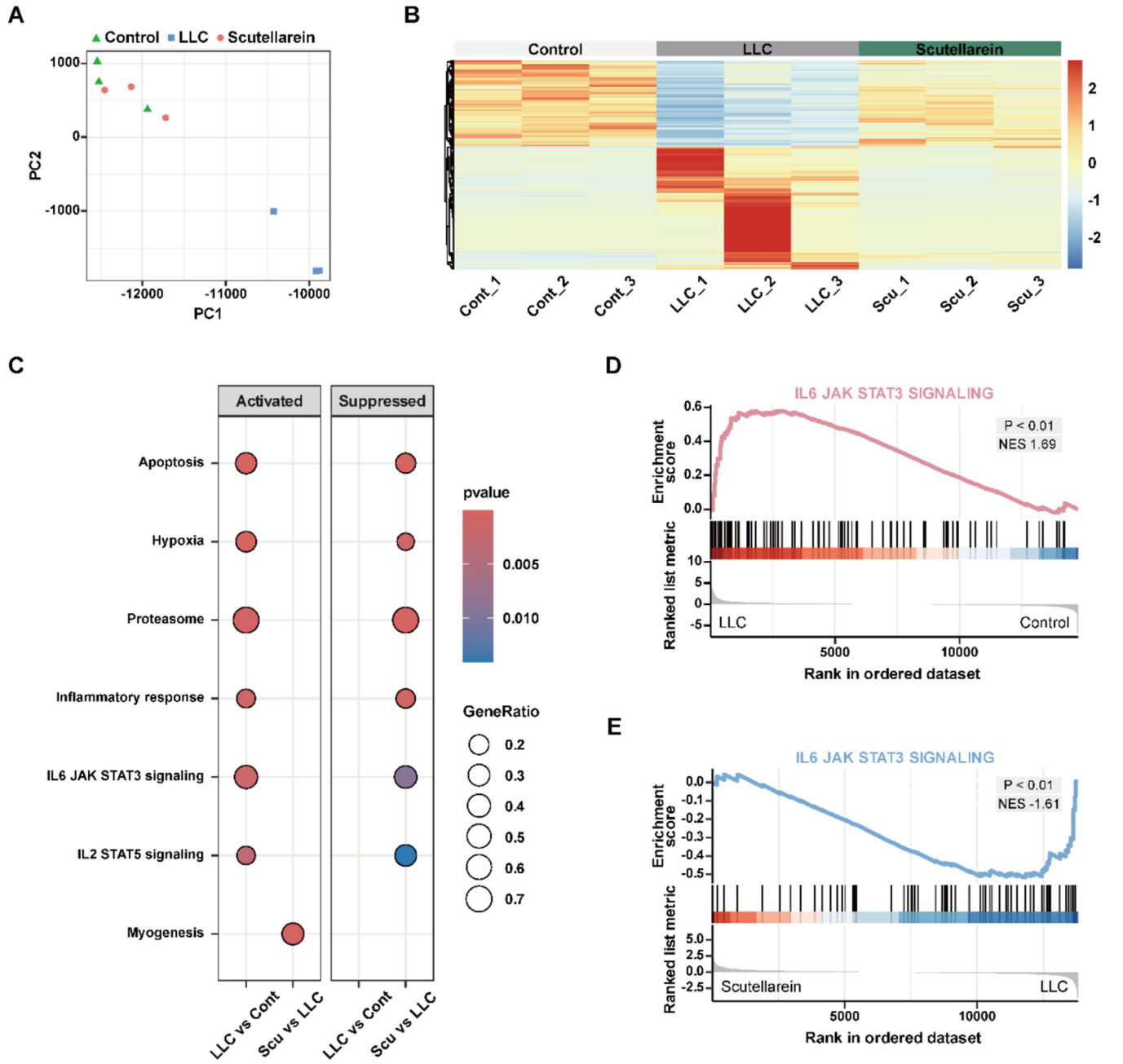

Fig. 6. The effect of scutellarein on cachexia-induced transcriptomic profiles in LLC-injected mice. To evaluate the impact of scutellarein on the transcriptomic profile of cachectic muscle, quadriceps muscles from LLC-induced cancer cachexia mice were subjected to RNA sequencing and analysis. (A) PCA plot visualizes the distribution of groups based on the first two principal components (PC1 and PC2), which together explain the majority of variance in the dataset. (B) Heatmap representation of differentially expressed genes (DEGs) between experimental groups, illustrating distinct clustering patterns. (C) Gene Set Enrichment Analysis (GSEA) was performed on the DEGs to identify significantly enriched hallmark and KEGG pathways among different groups (NES > 1, p-value < 0.05). (D,E) GSEA plot for JAK/STAT3 signaling pathway was illustrated for genes from (D) LLC group in comparison of control group, and (E) scutellarein group in comparison of LLC group, with statistical validation provided by both NES and p-values.

treated group showed significant downregulation of the JAK/STAT3 pathway, as reflected by the negative running enrichment scores (NES < –1.5, P < 0.01) (Fig. 6E). Transcriptomic profiling of cachectic muscles confirms that scutellarein effectively suppresses JAK/STAT3 signaling and counteracts cancer cachexia-associated muscle wasting, highlighting its potential as a therapeutic intervention.

Scutellarein protects human iPSC-derived skeletal muscle cells from IFN-γ/TNF-α-induced myotube atrophy

To further validate the efficacy of scutellarein in human muscle, the therapeutic effect of scutellarein was examined in human induced pluripotent stem cell (hiPSC)-derived skeletal muscle cells under inflammatory cachexia conditions. The hiPSC cells were differentiated into skeletal muscle cells for evaluation of scutellarein. Cells treated with pro-inflammatory cytokines IFN-γ and TNF-α exhibited significant thinning of myotubes and a marked reduction in the number of skeletal muscle cells, indicating myotube atrophy and degradation of myotube structure under inflammatory stress (Fig. 7A–C). However, treatment with scutellarein prior to inducing inflammatory stress preserved myotube diameter and increased the percentage of MHC-positive cells (Fig. 7A–C). This result was further confirmed through protein expression analysis of MHC (Fig. 7D). Furthermore, Titin expression was visibly higher in

scutellarein-treated cells compared to the atrophy-induced group, suggesting improved structural integrity and sarcomeric organization within the muscle fibers (Fig. 7E). Treatment with scutellarein did not display any observable cytotoxicity in hiPSC-derived skeletal muscle cells (Supplementary Fig. 6). JAK2 and STAT3 were activated in human skeletal muscle cells by inflammatory cytokines, then decreased by treatment with scutellarein (Fig. 7F). Together, these results indicate that scutellarein effectively counteracts IFN-γ/TNF-α-induced myotube atrophy in hiPSC-derived skeletal muscle cells by inhibiting the JAK2/STAT3 pathway and preserving myotube structure.

Hydroxyl group positioning in flavones determines inhibitory activity against JAK2

Scutellarein, also known as 4′,5,6,7-tetrahydroxyflavone, is a flavone characterized by four hydroxyl groups. To understand the structure–activity relationship of this compound, we prepared eight flavones that are structurally similar to scutellarein. Each of these flavones varies from scutellarein and from one another, containing either three or two of the hydroxyl groups found in scutellarein (Fig. 8A). Among these flavones, only baicalein exhibited similar inhibitory activity to scutellarein against JAK2 while the other flavones did not demonstrate significant activity towards JAK2 (Fig. 8B). Interestingly, scutellarein and baicalein were also found to effectively inhibit the downregulation of *Myod*, *Myogenin*, and *Pgc1a*, mediated by IFN-γ and TNF-α (Fig. 8C and D). Additionally, apigenin demonstrated similar effectiveness, consistent with previous studies that have shown apigenin's ability to enhance the expression of these genes through Prmt7 [41]. Furthermore, scutellarein and baicalein significantly inhibited the activation of STAT3, further supporting their role in suppressing JAK2 activity (Fig. 8E). Based on these results, it was inferred that the hydroxyl groups at carbons 5, 6, and 7 are critical for inhibiting JAK2.

To validate this conjecture, molecular docking was performed to explore the binding mechanism of scutellarein with JAK2. Several potential hydrogen bonds (indicated by dotted lines) were observed between scutellarein and JAK2 (Fig. 8F). To further confirm the predicted binding pose, we compared it with the experimental binding pose reported in the co-crystal structure of a known JAK2 imidazopyrrolopyridine inhibitor (Supplementary Fig. 7). The predicted pose of scutellarein overlayed well with the known compound. For the imidazopyrrolopyridine inhibitor, the two nitrogen atoms in the 1H-pyrrolo[2,3-b]pyridine ring formed bonds with the backbone carbonyl and amine groups of Glu930 and Leu932 in the hinge region of the kinase, respectively. Additionally, the delocalized π-electrons of the ring formed a CH-π interaction with Leu983 on the "floor" of the binding pocket. These typical kinase interactions were all replicated in the predicted binding pose of scutellarein (Fig. 8F and Supplementary Fig. 7), suggesting that the prediction is plausible. Based on the predicted binding pose, it can be observed that the hydroxyl group at position R4 extended outward from the binding pocket, failing to form any reliable interaction with key residues inside the pocket. This is consistent with the similar potency of scutellarein and baicalein, indicating that the absence of the hydroxyl group at R4 does not negatively affect the compound's potency (Fig. 8B). In contrast, the hydroxyl group at R1 is likely to form a hydrogen bond network with Gly993 and Asp994 via a water molecule observed from the co-crystal structure of 4F09, represented as a red sphere, suggesting its critical role in binding with the kinase (Fig. 8F). The absence of the hydroxyl at R1 significantly reduced inhibition, as observed when comparing baicalein to 5,6-dihydroxyflavone (Fig. 8B). Furthermore, potential hydrogen bonds were identified between the carbonyl group of Glu930 and the hydroxyl groups at R3 and R2, with the R3 hydroxyl group forming a potentially stronger hydrogen bond (2.9 Å) with the kinase, while the R2 hydroxyl group formed a weaker bond (3.5 Å) (Fig. 8F). This is in accordance with the inhibitory activity observed in previous experiments. Consequently, these results altogether suggest that the specific structure of scutellarein plays a key role in inhibiting JAK2, thereby preventing JAK2/STAT3 activation and mitigating muscle atrophy.

Discussion

The JAK2/STAT3 axis is activated by pro-inflammatory cytokines such as IL-6, IFN-γ, and TNF-α, which are elevated in cancer cachexia patients and contribute to muscle wasting by disrupting the balance between skeletal muscle protein synthesis and degradation [9,13,42]. Our findings demonstrate that scutellarein effectively inhibits JAK2 activity, preventing the downstream activation of STAT3. By blocking this pathway, scutellarein attenuates muscle wasting associated with cancer cachexia. These results suggest that scutellarein may serve as a novel therapeutic option in the treatment of cachexia, addressing a critical unmet need in the management of cancer-related morbidity.

Beyond its anti-cachectic effect, scutellarein has been reported to exert anti-inflammatory, antioxidant, and anti-cancer properties [17,18,43–48]. While these pleiotropic effects might be considered off-target in some therapeutic contexts, they may be advantageous in cancer cachexia, a complex systemic syndrome involving skeletal muscle atrophy, widespread inflammation, metabolic disruption, and adipose tissue depletion. In such multifactorial conditions, agents capable of modulating multiple pathogenic pathways simultaneously may offer therapeutic advantages over narrowly targeted drugs. For instance, in our study, scutellarein enhanced mitochondrial activity in muscle, consistent with its previously reported diverse beneficial effects. This observation is further supported by previous studies on the relationship between JAK/STAT pathway and mitochondrial function and biogenesis. STAT3 knockdown alleviates mitochondrial dysfunction and oxidative stress, while STAT3 suppresses PGC-1α expression and diminishes electron transport chain efficacy [49–51]. These findings support the mechanistic plausibility that inhibition of JAK2/STAT3 signaling by scutellarein contributes to improved mitochondrial function and energy metabolism in muscle. Collectively, these multiple therapeutic effects of scutellarein may offer substantial benefit in the management of cancer cachexia.

Despite the availability of several clinically approved JAK2 inhibitors, the identification of scutellarein introduces a novel candidate with distinct properties, particularly relevant to cancer cachexia [52]. While most existing JAK2 inhibitors were developed for hematologic malignancies and autoimmune disorders, scutellarein offers unique advantages in cachexia, its natural origin, pleiotropic activity, and favorable preclinical safety profile [53]. In our study, scutellarein demonstrated efficacy in both preventive and therapeutic cachexia models without detectable toxicity, supporting its potential suitability for long-term administration in vulnerable cancer patients. Unlike synthetic JAK inhibitors, which are often optimized for maximal potency but may present narrow therapeutic indices and off-target effects such as anemia, thrombocytopenia, or immunosuppression, scutellarein's moderate potency combined with its simultaneous actions on inflammation, mitochondrial biogenesis, and muscle protein homeostasis may offer a broader and safer therapeutic window well-suited for this multifactorial syndrome [54]. Also, the development of multiple inhibitors targeting the same molecule is a well-established drug development strategy, since it allows clinicians to tailor treatment

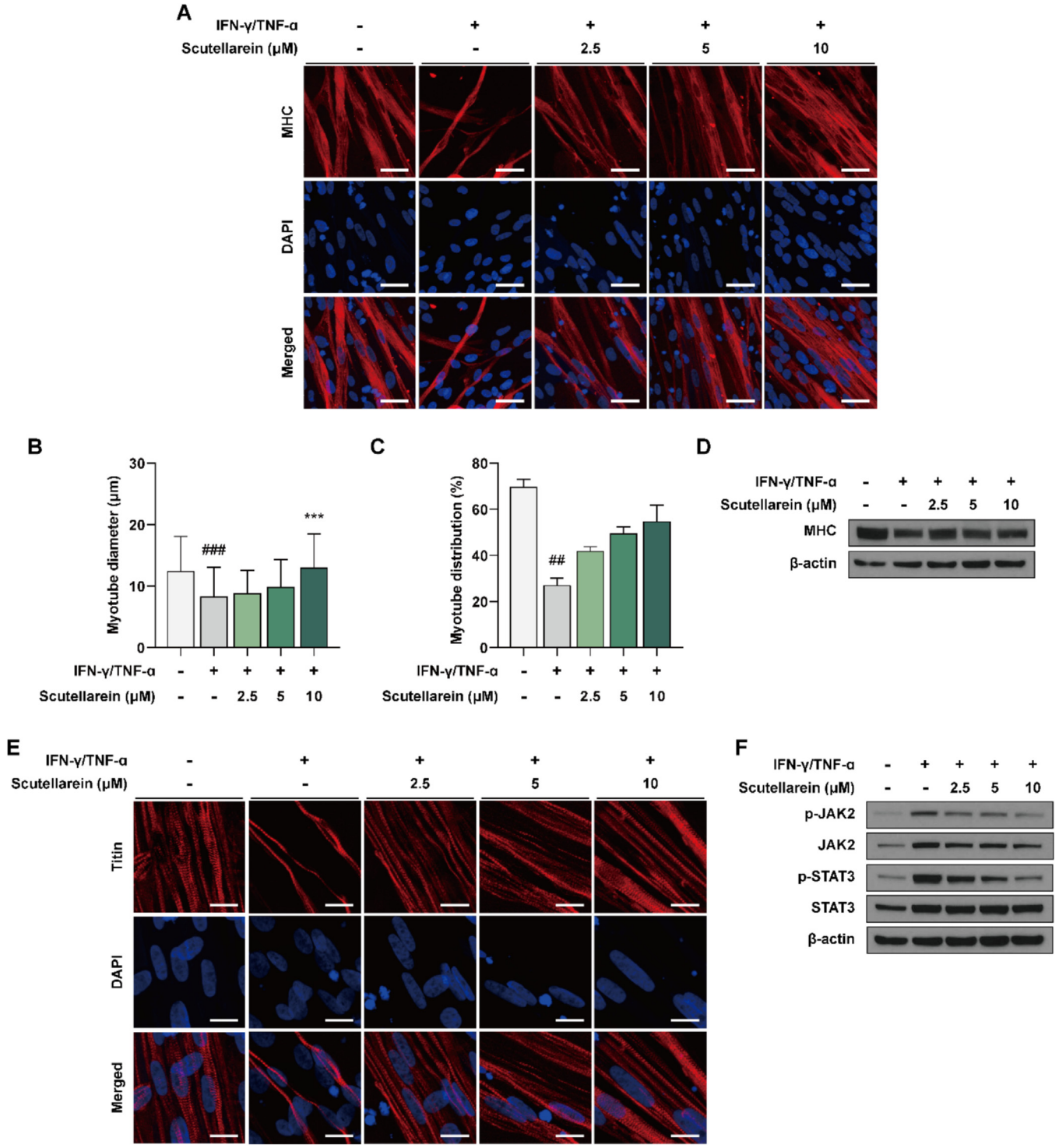

Fig. 7. Protective effects of scutellarein on human induced pluripotent stem cell (hiPSC)-derived skeletal muscle cells against IFN-γ/TNF-α-induced atrophy and inflammatory stress. hiPSC-derived skeletal muscle cells were treated with indicated concentrations of scutellarein and inflammatory cytokines, IFN-γ (100 ng/mL) and TNF-α (100 ng/mL). (A) Representative immunofluorescence images showing MHC (red), DAPI (blue), and merged images. Scale bar: 40 μm. (B-C) Quantification of (B) myotube diameter and (C) distribution based on MHC-stained images, analyzed using ImageJ software. (D) Immunoblot analysis of MHC protein expression levels. (E) Representative immunofluorescence images of Titin (red), DAPI (blue), and merged images. Scale bar: 40 μm. (F) Immunoblot analysis of phosphorylated and total JAK2 and STAT3. β-actin was used as a loading control. The data are presented as mean ± SD (n = 3). Statistical significance was determined by Kruskal-Wallis test followed by Dunnett's multiple comparisons test. ## $p < 0.01$ and ### $p < 0.001$ vs. control group; *** $p < 0.001$ vs. IFN-γ/TNF-α group. (For interpretation of the references to colour in this figure legend, the reader is referred to the web version of this article.)

based on patient-specific needs, as exemplified by EGFR and JAK inhibitor classes [52,55–57]. In this context, identification of natural compounds such as scutellarein expands the therapeutic landscape and may serve as a foundation for further optimization.

Furthermore, our study is the first to demonstrate the direct inhibitory activity of scutellarein against JAK and to define its unique structural basis for target engagement. Previous studies have examined scutellarin, a glycosylated derivative of scutel-

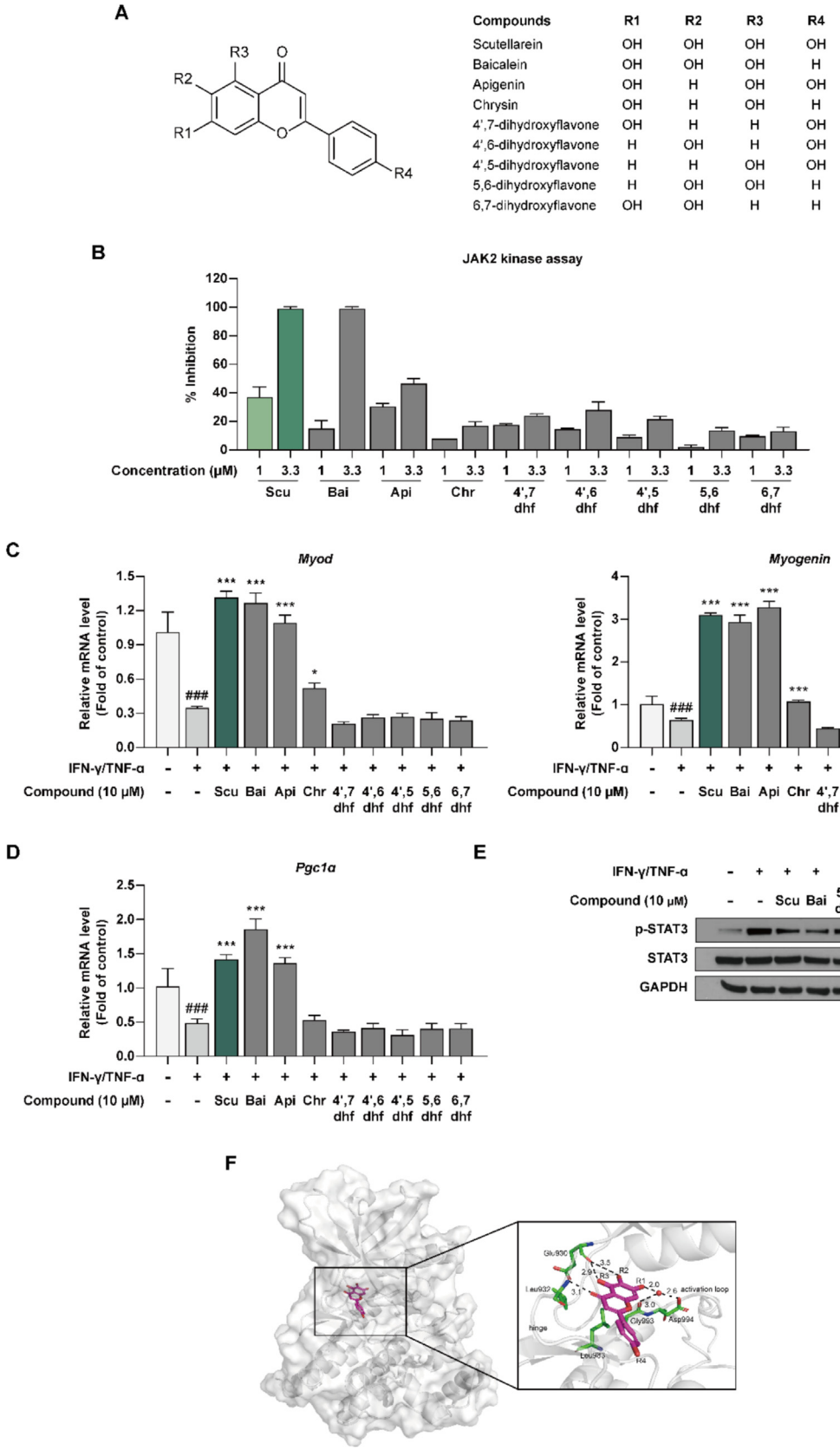
A
R3
O
R2
R1
O
R4
Compounds R1 R2 R3 R4
Scutellarein OH OH OH OH
Baicalein OH OH OH H
Apigenin OH H OH OH
Chrysin OH H OH H
4',7-dihydroxyflavone OH H H OH
4',6-dihydroxyflavone H OH H OH
4',5-dihydroxyflavone H H OH OH
5,6-dihydroxyflavone H OH OH H
6,7-dihydroxyflavone OH OH H H
B
JAK2 kinase assay
% Inhibition
Concentration (μM) 1 3.3 1 3.3 1 3.3 1 3.3 1 3.3 1 3.3 1 3.3 1 3.3 1 3.3
Scu Bai Api Chr 4',7 dhf 4',6 dhf 4',5 dhf 5,6 dhf 6,7 dhf
C
Myod
Myogenin
Relative mRNA level (Fold of control)
IFN-γ/TNF-α
Compound (10 μM)
Scu Bai Api Chr 4',7 dhf 4',6 dhf 4',5 dhf 5,6 dhf 6,7 dhf
D
Pgc1α
E
IFN-γ/TNF-α
Compound (10 μM)
Scu Bai 5,6 dhf 6,7 dhf
p-STAT3
STAT3
GAPDH
F
Glu930
Leu932
hinge
Gly993
Asp994
activation loop
Leu983
R4

larein, reporting modulation of JAK/STAT signaling; however, these effects were inconsistent, context-dependent, and typically required high concentrations, with no direct biochemical evidence of JAK inhibition [58–61]. In addition, glycosylation and subtle structural modifications are known to significantly alter bioactivity, pharmacokinetics, and target interactions. In contrast, our data show that scutellarein directly inhibits JAK kinase activity, as demonstrated by *in vitro* kinase assays, Kd determination, molecular docking, and suppression of JAK2/STAT3 phosphorylation in both *in vitro* and in vivo models. Such structure–activity relationship analysis further differentiates scutellarein from related flavonoids by identifying key hydroxylation patterns necessary for JAK2 binding. Collectively, these findings establish scutellarein as a novel direct JAK inhibitor with therapeutic relevance for cancer cachexia, a condition for which no JAK-targeted therapy has been optimized to date.

These findings also have important translational implications, highlighting the potential of scutellarein for clinical application. By inhibiting the JAK/STAT pathway, scutellarein may help preserve muscle mass, improve quality of life, and enhance survival rates in cancer patients suffering from cachexia. In our study, scutellarein demonstrated efficacy in two animal models and exhibited positive effects in human muscle cells, further supporting its translational potential. Additionally, as a natural compound, scutellarein holds appeal for long-term administration in patients and offers additional potential for development into medical or functional food products [62]. However, to advance these findings toward clinical application, further studies are needed to determine the optimal dosage, administration routes, and long-term safety. Comprehensive toxicity studies and pharmacokinetic/pharmacodynamic profiling will be essential to fully characterize its in vivo behavior and safety profile.

Conclusions

In conclusion, our study identifies a natural compound scutellarein as a JAK inhibitor that counteracts cancer cachexia by inhibiting the JAK2/STAT3 pathway. Scutellarein preserves muscle structure, enhances mitochondrial function, and prevents muscle wasting in cell and animal models, offering a potential therapeutic strategy.

Compliance with ethics requirements

All human participants gave their informed consent for the scientific use of their samples, and all procedures involving human samples were approved by the Institutional Review Board of Severance Hospital (IRB No. 4-2018-0890).

All animal experiments and methodologies employed in this research were approved by the Seoul Women's University Animal Care and Use Committee (SWU IACUC 2023A-17).

CRediT authorship contribution statement

Heeju Ahn: Writing – original draft, Data curation, Formal analysis. **Heeju Kim:** Writing – original draft & editing, Data curation, Formal analysis. **Yeyoung Yoon:** Data curation, Investigation. **Minju Jeong:** Data curation, Investigation. **Sieun Lee:** Data curation, Investigation. **Peng Chen:** Data curation, Investigation. **Keke Wang:** Data curation, Investigation. **Sujung Park:** Data curation. **Jae Hwan Kim:** Data curation. **Jiyun Ahn:** Data curation. **Qiantao Wang:** Supervision. **Yoonhee Jin:** Supervision. **Young Jin Jang:** Conceptualization, Resources, Supervision. **Sanguine Byun:** Conceptualization, Resources, Writing – review & editing, Supervision.

Declaration of competing interest

The authors declare that they have no known competing financial interests or personal relationships that could have appeared to influence the work reported in this paper.

Acknowledgments

This study was supported by grants from the National Research Foundation of Korea (NRF) grant funded by the Korea government (MSIT) (No. RS-2023-00222997 and 2023R1A2C1006827 (NR076822), Republic of Korea) and Seoul Women's University (No. 2025-0184, Republic of Korea). H. Kim is a fellowship awardee by the Brain Korea 21 (BK21) FOUR program.

Appendix A. Supplementary data

Supplementary data to this article can be found online at https://doi.org/10.1016/j.jare.2025.07.001.

References

[1] Ni J, Zhang L. Cancer cachexia: definition, staging, and emerging treatments. Cancer Manag Res 2020:5597–605. doi: https://doi.org/10.2147/CMAR.S261585.
[2] Wyart E, Carrà G, Angelino E, Penna F, Porporato PE. Systemic metabolic crosstalk as driver of cancer cachexia. Trends Endocrinol Metab 2025. doi: https://doi.org/10.1016/j.tem.2024.12.005.
[3] Siff T, Parajuli P, Razzaque MS, Atfi A. Cancer-mediated muscle cachexia: etiology and clinical management. Trends Endocrinol Metab 2021;32(6):382–402. doi: https://doi.org/10.1016/j.tem.2021.03.007.
[4] Argilés JM, Busquets S, Stemmler B, López-Soriano FJ. Cancer cachexia: understanding the molecular basis. Nat Rev Cancer 2014;14(11):754–62. doi: https://doi.org/10.1038/nrc3829.
[5] Wallengren O, Lundholm K, Bosaeus I. Diagnostic criteria of cancer cachexia: relation to quality of life, exercise capacity and survival in unselected palliative care patients. Support Care Cancer 2013;21:1569–77. doi: https://doi.org/10.1007/s00520-012-1697-z.
[6] Faiad J, Andrade MF, de Castro G, de Resende J, Coêlho M, Aquino G, et al. Muscle loss in cancer cachexia: what is the basis for nutritional support? Front Pharmacol 2025;16:1519278. doi: https://doi.org/10.3389/fphar.2025.1519278.
[7] de Castro GS, Simoes E, Lima JD, Ortiz-Silva M, Festuccia WT, Tokeshi F, et al. Human cachexia induces changes in mitochondria, autophagy and apoptosis in the skeletal muscle. Cancers 2019;11(9):1264. doi: https://doi.org/10.3390/cancers11091264.
[8] Pijet B, Pijet M, Litwiniuk A, Gajewska M, Pająk B, Orzechowski A. TNF-α and IFN-s-dependent muscle decay is linked to NF-κB-and STAT-1α-stimulated atrogin1 and MuRF1 genes in C2C12 myotubes. Mediat Inflamm 2013;2013(1):171437. doi: https://doi.org/10.1155/2013/171437.
[9] Ma JF, Sanchez BJ, Hall DT, Tremblay AMK, Di Marco S, Gallouzi IE. STAT 3 promotes IFN γ/TNF α-induced muscle wasting in an NF-κB-dependent and IL-6-independent manner. EMBO Mol Med 2017;9(5):622–37. doi: https://doi.org/10.15252/emmm.201607052.

Fig. 8. Hydroxyl group positioning in flavones modulates JAK2 inhibition and STAT3 signaling. (A) Chemical structures of scutellarein and eight structurally related flavones. The structures of scutellarein and eight flavones, each containing two or three hydroxyl groups located at carbons 4′, 5, 6, and 7, are presented. (B) Inhibitory effects of scutellarein and eight flavones on JAK2 activity. The JAK2 kinase assay results for scutellarein and eight structurally related flavones are shown. Each flavone was tested at concentrations of 1 μM and 3.3 μM to evaluate their inhibitory effects on JAK2. (C-E) Myotubes were treated with flavones (10 μM) and inflammatory cytokines, IFN-γ (20 ng/mL) and TNF-α (20 ng/mL). The mRNA expression of (C) MyoD, myogenin, and (D) PGC-1α was evaluated by qRT-PCR. (E) Expression levels of phosphorylated and total STAT3 were analyzed by immunoblotting. GAPDH was used as a loading control. (F) Predicted binding pose of scutellarein with JAK2 (PDB ID: 4F09). The compound is shown in magenta, while the protein is in silver cartoon and key residues in green sticks. A water molecule taken from the crystal structure was shown as a small red sphere. Statistical significance was determined by one-way ANOVA followed by Dunnett's multiple comparisons test. ### $p < 0.001$ vs. control group; * $p < 0.05$ and *** $p < 0.001$ vs. IFN-γ/TNF-α group. (For interpretation of the references to colour in this figure legend, the reader is referred to the web version of this article.)

[10] Riccardi DMDR, das Neves RX, de Matos-Neto EM, Camargo RG, Lima JDCC, Radloff K, et al. Plasma lipid profile and systemic inflammation in patients with cancer cachexia. Front Nutr 2020;7:4. doi: https://doi.org/10.3389/fnut.2020.00004.
[11] Matsuyama T, Ishikawa T, Okayama T, Oka K, Adachi S, Mizushima K, et al. Tumor inoculation site affects the development of cancer cachexia and muscle wasting. Int J Cancer 2015;137(11):2558–65. doi: https://doi.org/10.1002/ijc.29620.
[12] Bonetto A, Aydogdu T, Kunzevitzky N, Guttridge DC, Khuri S, Koniaris LG, et al. STAT3 activation in skeletal muscle links muscle wasting and the acute phase response in cancer cachexia. PLoS One 2011;6(7):e22538. doi: https://doi.org/10.1371/journal.pone.0022538.
[13] Bonetto A, Aydogdu T, Jin X, Zhang Z, Zhan R, Puzis L, et al. JAK/STAT3 pathway inhibition blocks skeletal muscle wasting downstream of IL-6 and in experimental cancer cachexia. Am J Physiol-Endocrinol Metab 2012;303(3):E410–21. doi: https://doi.org/10.1152/ajpendo.00039.2012.
[14] Arora GK, Gupta A, Guo T, Gandhi AY, Laine A, Williams DL, et al. JAK inhibitors suppress cancer cachexia-associated anorexia and adipose wasting in mice. JCSM Rapid Commun 2020;3(2):115–28. doi: https://doi.org/10.1002/rco2.24.
[15] Atanasov AG, Zotchev SB, Dirsch VM, Supuran CT. Natural products in drug discovery: advances and opportunities. Nat Rev Drug Discov 2021;20(3):200–16. doi: https://doi.org/10.1038/s41573-020-00114-z.
[16] Lin Y, Ren N, Li S, Chen M, Pu P. Novel anti-obesity effect of scutellarein and potential underlying mechanism of actions. Biomed Pharmacother 2019;117:109042. doi: https://doi.org/10.1016/j.biopha.2019.109042.
[17] Park MY, Ha SE, Kim HH, Bhosale PB, Abusaliya A, Jeong SH, et al. Scutellarein inhibits LPS-induced inflammation through NF-κB/MAPKs signaling pathway in RAW264. 7 cells. Molecules 2022;27(12):3782. doi: https://doi.org/10.3390/molecules27123782.
[18] Sung NY, Kim MY, Cho JY. Scutellarein reduces inflammatory responses by inhibiting Src kinase activity. Korean J Physiol Pharmacol 2015;19(5):441. doi: https://doi.org/10.4196/kjpp.2015.19.5.441.
[19] Trott O, Olson AJ. AutoDock Vina: improving the speed and accuracy of docking with a new scoring function, efficient optimization, and multithreading. J Comput Chem 2010;31(2):455–61. doi: https://doi.org/10.1002/jcc.21334.
[20] Schmidt EK, Clavarino G, Ceppi M, Pierre P. SUnSET, a nonradioactive method to monitor protein synthesis. Nat Methods 2009;6(4):275–7. doi: https://doi.org/10.1038/nmeth.1314.
[21] Ahn J, Kim MJ, Ahn J, Ha TY, Jung CH, Seo HD, et al. Identifying Codium fragile extract components and their effects on muscle weight and exercise endurance. Food Chem 2021;353:129463. doi: https://doi.org/10.1016/j.foodchem.2021.129463.
[22] Mengie Ayele T, Tilahun Muche Z, Behaile Teklemariam A, Bogale Kassie A, Chekol Abebe E. Role of JAK2/STAT3 signaling pathway in the tumorigenesis, chemotherapy resistance, and treatment of solid tumors: a systemic review. J Inflamm Res 2022:1349–64. doi: https://doi.org/10.2147/JIR.S353489.
[23] Siddiqui JA, Pothuraju R, Jain M, Batra SK, Nasser MW. Advances in cancer cachexia: intersection between affected organs, mediators, and pharmacological interventions. Biochim Biophys Acta Rev Cancer 2020;1873(2):188359. doi: https://doi.org/10.1016/j.bbcan.2020.188359.
[24] Langen RC, Schols AM, Kelders MC, Wouters EF, Janssen-Heininger YM. Inflammatory cytokines inhibit myogenic differentiation through activation of nuclear factor-κB. FASEB J 2001;15(7):1169–80. doi: https://doi.org/10.1096/fj.00-0463.
[25] Londhe P, Davie JK. Gamma interferon modulates myogenesis through the major histocompatibility complex class II transactivator, CIITA. Mol Cell Biol 2011;31(14):2854–66. doi: https://doi.org/10.1128/MCB.05397-11.
[26] Wagner KU, Rui H. Jak2/Stat5 signaling in mammogenesis, breast cancer initiation and progression. J Mammary Gland Biol Neoplasia 2008;13:93–103. doi: https://doi.org/10.1007/s10911-008-9062-z.
[27] Noë S, Corvelyn M, Willems S, Costamagna D, Aerts JM, Van Campenhout A, et al. The Myotube Analyzer: how to assess myogenic features in muscle stem cells. Skelet Muscle 2022;12(1):12. doi: https://doi.org/10.1186/s13395-022-00297-6.
[28] Comai G, Tajbakhsh S. Molecular and cellular regulation of skeletal myogenesis. Curr Top Dev Biol 2014;110:1–73. doi: https://doi.org/10.1016/B978-0-12-405943-6.00001-4.
[29] Hernández-Hernández JM, García-González EG, Brun CE, Rudnicki MA. The myogenic regulatory factors, determinants of muscle development, cell identity and regeneration. Semin Cell Dev Biol 2017;72:10–8. doi: https://doi.org/10.1016/j.semcdb.2017.11.010.
[30] Bodine SC, Baehr LM. Skeletal muscle atrophy and the E3 ubiquitin ligases MuRF1 and MAFbx/atrogin-1. Am J Physiol-Endocrinol Metab 2014;307(6):E469–84. doi: https://doi.org/10.1152/ajpendo.00204.2014.
[31] Huang Z, Zhong L, Zhu J, Xu H, Ma W, Zhang L, et al. Inhibition of IL-6/JAK/STAT3 pathway rescues denervation-induced skeletal muscle atrophy. Ann Transl Med 2020;8(24). doi: https://doi.org/10.21037/atm-20-7269.
[32] Goodman CA. The role of mTORC1 in regulating protein synthesis and skeletal muscle mass in response to various mechanical stimuli. Rev Physiol Biochem Pharmacol 2014;166:43–95. doi: https://doi.org/10.1007/112_2013_17.
[33] Bodine SC, Stitt TN, Gonzalez M, Kline WO, Stover GL, Bauerlein R, et al. Akt/mTOR pathway is a crucial regulator of skeletal muscle hypertrophy and can prevent muscle atrophy in vivo. Nat Cell Biol 2001;3(11):1014–9. doi: https://doi.org/10.1038/ncb1101-1014.
[34] Jeon SM. Regulation and function of AMPK in physiology and diseases. Exp Mol Med 2016;48(7):e245–e. doi: https://doi.org/10.1038/emm.2016.81.
[35] Wang P, Liu J, Li Y, Wu S, Luo J, Yang H, et al. Peroxisome proliferator-activated receptor δ is an essential transcriptional regulator for mitochondrial protection and biogenesis in adult heart. Circ Res 2010;106(5):911–9. doi: https://doi.org/10.1161/CIRCRESAHA.109.206185.
[36] Cohen S, Nathan JA, Goldberg AL. Muscle wasting in disease: molecular mechanisms and promising therapies. Nat Rev Drug Discov 2015;14(1):58–74. doi: https://doi.org/10.1038/nrd4467.
[37] Sandri M. Protein breakdown in cancer cachexia. Semin Cell Dev Biol 2016;54:11–9. doi: https://doi.org/10.1016/j.semcdb.2015.11.002.
[38] Tsoli M, Swarbrick MM, Robertson GR. Lipolytic and thermogenic depletion of adipose tissue in cancer cachexia. Semin Cell Dev Biol 2016;54:68–81. doi: https://doi.org/10.1016/j.semcdb.2015.10.039.
[39] Fedorenko A, Lishko PV, Kirichok Y. Mechanism of fatty-acid-dependent UCP1 uncoupling in brown fat mitochondria. Cell 2012;151(2):400–13. doi: https://doi.org/10.1016/j.cell.2012.09.010.
[40] Sakuma K, Yamaguchi A. Sarcopenia and cachexia: the adaptations of negative regulators of skeletal muscle mass. J Cachexia Sarcopenia Muscle 2012;3:77–94. doi: https://doi.org/10.1007/s13539-011-0052-4.
[41] Jang YJ, Son HJ, Choi YM, Ahn J, Jung CH, Ha TY. Apigenin enhances skeletal muscle hypertrophy and myoblast differentiation by regulating Prmt7. Oncotarget 2017;8(45):78300. doi: https://doi.org/10.18632/oncotarget.20962.
[42] Miyamoto Y, Hanna DL, Zhang W, Baba H, Lenz HJ. Molecular pathways: cachexia signaling—a targeted approach to cancer treatment. Clin Cancer Res 2016;22(16):3999–4004. doi: https://doi.org/10.1158/1078-0432.CCR-16-0495.
[43] Li X, Zhang X, Kang Y, Cai M, Yan J, Zang C, et al. Scutellarein suppresses the production of ROS and inflammatory mediators of LPS-activated bronchial epithelial cells and attenuates acute lung injury in mice. Antioxidants 2024;13(6):710. doi: https://doi.org/10.3390/antiox13060710.
[44] Qian LH, Li NG, Tang YP, Zhang L, Tang H, Wang ZJ, et al. Synthesis and bioactivity evaluation of scutellarein as a potent agent for the therapy of ischemic cerebrovascular disease. Int J Mol Sci 2011;12(11):8208–16. doi: https://doi.org/10.3390/ijms12118208.
[45] Spiegel M, Marino T, Prejanò M, Russo N. On the scavenging ability of scutellarein against the OOH radical in water and lipid-like environments: a theoretical study. Antioxidants 2022;11(2):224. doi: https://doi.org/10.3390/antiox11020224.
[46] Shi L, Wu Y, Feng L. Scutellarein selectively targets multiple myeloma cells by increasing mitochondrial superoxide production and activating intrinsic apoptosis pathway. Biomed Pharmacother 2019;109:2109–18. doi: https://doi.org/10.1016/j.biopha.2018.09.024.
[47] Shi X, Chen G, Liu X, Qiu Y, Yang S, Zhang Y, et al. Scutellarein inhibits cancer cell metastasis in vitro and attenuates the development of fibrosarcoma in vivo. Int J Mol Med 2015;35(1):31–8. doi: https://doi.org/10.3892/ijmm.2014.1997.
[48] Lang X, Chen Z, Yang X, Yan Q, Xu M, Liu W, et al. Scutellarein induces apoptosis and inhibits proliferation, migration, and invasion in ovarian cancer via inhibition of EZH2/FOXO1 signaling. J Biochem Mol Toxicol 2021;35(10):e22870. doi: https://doi.org/10.1002/jbt.22870.
[49] Peng D, He X, Ren B, Wang Q, Peng L, Jiang Y, et al. JAK2/STAT3/HMGCS2 signaling aggravates mitochondrial dysfunction and oxidative stress in hyperuricemia-induced cardiac dysfunction. Mol. Med. 2025;31(1):1–23. doi: https://doi.org/10.1186/s10020-025-01246-x.
[50] Liu S, Li W, Liang L, Zhou Y, Li Y. The regulatory relationship between transcription factor STAT3 and noncoding RNA. Cell Mol Biol Lett 2024;29(1):4. doi: https://doi.org/10.1186/s11658-023-00521-1.
[51] Richardson PJ, Smith DP, de Giorgio A, Snetkov X, Almond-Thynne J, Cronin S, et al. Janus kinase inhibitors are potential therapeutics for amyotrophic lateral sclerosis. Eurodegener 2023;12(1):47. doi: https://doi.org/10.1186/s40035-023-00380-y.
[52] Verstovsek S. Therapeutic potential of JAK2 inhibitors. Am Soc Hematol Educ Program 2009;2009(1):636–42. doi: https://doi.org/10.1182/asheducation-2009.1.636.
[53] Vainchenker W, Dusa A, Constantinescu SN. JAKs in pathology: role of Janus kinases in hematopoietic malignancies and immunodeficiencies. Semin Cell Dev Biol 2008;19(4):385–93. doi: https://doi.org/10.1016/j.semcdb.2008.07.002.
[54] Vainchenker W, Leroy E, Gilles L, Marty C, Plo I, Constantinescu SN. JAK inhibitors for the treatment of myeloproliferative neoplasms and other disorders. F1000Res 2018;7:82. doi: https://doi.org/10.12688/f1000research.13167.1.
[55] Suzumura T, Kimura T, Kudoh S, Umekawa K, Nagata M, Matsuura K, et al. Reduced CYP2D6 function is associated with gefitinib-induced rash in patients with non-small cell lung cancer. BMC Cancer 2012;12:1–9. doi: https://doi.org/10.1186/1471-2407-12-568.
[56] Soria JC, Ohe Y, Vansteenkiste J, Reungwetwattana T, Chewaskulyong B, Lee KH, et al. Osimertinib in untreated EGFR-mutated advanced non–small-cell lung cancer. N Engl J Med 2018;378(2):113–25. doi: https://doi.org/10.1056/NEJMoa1713137.
[57] He J, Huang Z, Han L, Gong Y, Xie C. Mechanisms and management of 3rd generation EGFR TKI resistance in advanced non small cell lung cancer. Int J Oncol 2021;59(5):1–20. doi: https://doi.org/10.3892/ijo.2021.5270.

[58] Duan ZD, Zheng LY, Jia QY, Chen HL, Xu DY, Yang YJ, et al. Effect of scutellarin on BV-2 microglial-mediated apoptosis in PC12 cells via JAK2/STAT3 signalling pathway. Sci Rep 2024;14(1):13430. doi: https://doi.org/10.1038/s41598-024-64226-x.
[59] Liu K, Tian T, Zheng Y, Zhou L, Dai C, Wang M, et al. Scutellarin inhibits proliferation and invasion of hepatocellular carcinoma cells via down-regulation of JAK2/STAT3 pathway. J Cell Mol Med 2019;23(4):3040–4. doi: https://doi.org/10.1111/jcmm.14169.
[60] Jia QY, Chen HL, Qi Z, Zhang XLN, Zheng LY, Liu TT, et al. Network pharmacology to explore the mechanism of scutellarin in the treatment of brain ischaemia and experimental verification of JAK2/STAT3 signalling pathway. Sci Rep 2023;13(1):7557. doi: https://doi.org/10.1038/s41598-023-33156-5.
[61] Wang T, Liu B, Huang J, Zhao Q, Shen H, Bi T, et al. IFN-γ-mediated inhibition of JAK/STAT signaling via nano-scutellarin treatment is an efficient strategy for ameliorating liver fibrosis. J Transl Med 2025;23(1):195. doi: https://doi.org/10.1186/s12967-025-06155-5.
[62] Mondal S, Soumya NPP, Mini S, Sivan SK. Bioactive compounds in functional food and their role as therapeutics. Bioact Compd Health Dis 2021;4(3):24–39. doi: https://doi.org/10.31989/bchd.v4i3.786.